



## Synthesis of niobium borides by powder metallurgy methods using $\text{Nb}_2\text{O}_5$ , $\text{B}_2\text{O}_3$ and Mg blends

Özge Balcı, Duygu Ağaoğulları, M. Lütfi Öveçoğlu, İsmail Duman

Faculty of Chemical and Metallurgical Engineering, Department of Metallurgical and Materials Engineering, Particulate Materials Laboratories, İstanbul Technical University, Ayazağa Campus, 34469 Maslak, İstanbul, Turkey

Received 15 April 2015; accepted 21 August 2015

**Abstract:** Niobium boride powders having NbB, NbB<sub>2</sub> and Nb<sub>3</sub>B<sub>4</sub> phases in various amounts and single phase NbB powders were successfully synthesized by using powder metallurgy methods from related metal oxide raw materials in the presence of a strong reducing agent. Nb<sub>2</sub>O<sub>5</sub>, B<sub>2</sub>O<sub>3</sub> and Mg powder blends were milled at room temperature by a high-energy ball mill for different time. Subsequently, undesired MgO phase was removed from the milled powders by HCl leaching to constitute NbB–NbB<sub>2</sub>–Nb<sub>3</sub>B<sub>4</sub> as final products and they were subjected to an annealing process at 1500 °C for 4 h to observe probable boride transformation. Characterization was carried out by XRD, DSC, PSA, SEM/EDX, TEM and VSM. The effects of milling time (up to 9 h) on the formation, microstructure and thermal behavior of the final products were investigated. Reduction reaction took place after milling stoichiometric powder blends for 2 h. Nano-sized NbB–NbB<sub>2</sub>–Nb<sub>3</sub>B<sub>4</sub> powders in high purity were obtained in the absence of any secondary phase and any impurity via mechanochemistry by milling for 5 h and leaching with 4 mol/L HCl. After annealing, pure and nano-sized NbB–NbB<sub>2</sub>–Nb<sub>3</sub>B<sub>4</sub> powders transformed to a single NbB phase without leaving behind NbB<sub>2</sub> and Nb<sub>3</sub>B<sub>4</sub> phases.

**Key words:** niobium boride powders; powder metallurgy; mechanochemical synthesis; annealing; microstructure

### 1 Introduction

Niobium borides are well known for their high melting point (~3000 °C), high strength, high chemical stability and high thermal and electrical conductivity [1–3]. According to the proposed binary phase diagrams of Nb–B system, six types of niobium borides have been reported [1,4,5]. In general, there is an agreement in the archival literature regarding the stability of the NbB, Nb<sub>3</sub>B<sub>4</sub> and NbB<sub>2</sub> phases, whereas the stabilities of Nb<sub>3</sub>B<sub>2</sub>, Nb<sub>5</sub>B<sub>6</sub> and Nb<sub>2</sub>B<sub>3</sub> phases are arguable [6]. The crystal structures of the NbB<sub>2</sub>, Nb<sub>3</sub>B<sub>4</sub>, Nb<sub>5</sub>B<sub>6</sub>, NbB and Nb<sub>3</sub>B<sub>2</sub> phases are of AlB<sub>2</sub>, Ta<sub>3</sub>B<sub>4</sub>, V<sub>5</sub>B<sub>6</sub>, CrB and U<sub>3</sub>Si<sub>2</sub> types, respectively [7]. NbB<sub>2</sub> exhibits a hexagonal structure with a space group of *P6/mmm*, in which Nb and B atoms occupy the 1a and 2d positions, respectively [6,7]. Nb<sub>3</sub>B<sub>4</sub> has the orthorhombic structure with a space group of *Immm*, in which Nb atoms occupy 2c and 4g positions and B atoms occupy 4g and 4h positions [6,7]. NbB has the orthorhombic structure with a space group of *Cmcm*, in which Nb and B atoms are in the 4c positions [6,7].

Superconducting behavior of niobium borides has

been investigated in many reports for many years [8,9]. These studies generally revealed that stoichiometric niobium diboride did not have superconductivity down to very low temperatures whereas non-stoichiometric niobium borides had superconductivity at different transition temperatures [10–12]. Therefore, non-stoichiometric compounds of niobium borides have been a matter in many research studies as potential superconductors [8,11]. Furthermore, niobium borides are recognized as probable candidates for high temperature structural applications and they are known as refractory and coating materials which have excellent oxidation stability at high temperatures [13].

Many processes are available for the fabrication of niobium borides such as high temperature methods using solid state reactions, borothermal and carbothermal reductions [14–21], low-temperature synthesis in an autoclave [22,23], self-propagating high-temperature synthesis (SHS) [3,10,24–26], chemical vapor deposition (CVD) [13], ball milling and mechanochemical synthesis [27–30]. Borothermal and carbothermal reductions require reaction temperatures above 1600 °C to obtain the niobium boride phases by using Nb<sub>2</sub>O<sub>5</sub> and

B/B<sub>2</sub>O<sub>3</sub> as starting materials [14,15,21]. Solid state reactions were carried out using arc furnace or RF thermal plasma source, starting from Nb and B elemental powders [16,17,20]. NbB<sub>2</sub> nanorods and nanocrystals were prepared from chloride-based raw materials at low temperatures (500–600 °C) using an autoclave [22,23]. SHS processes were conducted using Nb/B and Nb<sub>2</sub>O<sub>5</sub>/B powder mixtures and non-stoichiometric phases of niobium boride were obtained instead of a single NbB<sub>2</sub> phase [10,24–26]. NbB<sub>2</sub> was deposited on a quartz substrate by chemical vapor deposition using gas mixtures of NbCl<sub>5</sub>, BCl<sub>3</sub> and H<sub>2</sub> in the temperature range of 950–1200 °C resulting in the occurrence of homogeneous films between 950 and 1050 °C and pillar crystals between 1050 and 1200 °C during precipitation step of the process [13]. Ball milling and mechanochemical synthesis were recently utilized for the preparation of niobium borides. However, these processes were reported with the mechanical alloying of Nb and B elemental powders or mechanochemistry of Nb–B<sub>2</sub>O<sub>3</sub>–Mg powder blends [27–30].

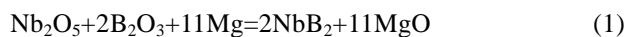
The application of high temperatures, the use of expensive starting materials (elemental Nb or B) and/or the use of complicated equipments may restrict the fabrication process to obtain niobium borides for the demanded applications. Mechanochemistry route utilized in this study was enabled to prepare niobium boride powders with high efficiency, small particle size and high purity by using low cost oxide raw materials.

In this study, niobium boride powders having NbB, NbB<sub>2</sub> and Nb<sub>3</sub>B<sub>4</sub> phases in various amounts and single phase NbB powders were synthesized by using powder metallurgy methods from Nb<sub>2</sub>O<sub>5</sub>, B<sub>2</sub>O<sub>3</sub> and Mg powder blends. Effects of milling time on the formation, microstructure and thermal behavior of the final products were investigated. This study contributes to the literature as the first results of a novel and simple process which enables the formation of the pure niobium boride powders from oxide reactants at room temperature thanks to the effect of mechanical milling.

## 2 Experimental

Niobium oxide (Nb<sub>2</sub>O<sub>5</sub>, Alfa Aesar<sup>TM</sup>, purity 99.5%, average particle size 150 μm), boron oxide (B<sub>2</sub>O<sub>3</sub>, ETI Mine, purity 98%, average particle size 467 μm) powders as oxide raw materials and magnesium powders (Mg, MME, purity 99.7%, average particle size 112 μm) as reducing agent were used. Powder blends containing stoichiometric amounts of reactants were prepared according to the theoretical reduction reaction given in Eq. (1). However, it is already known that the complete reduction of Nb<sub>2</sub>O<sub>5</sub> to NbB<sub>2</sub> could not be possible considering the presence of six different types of

niobium borides in the range of 40%–70% B, in the binary Nb–B phase diagram and also non-equilibrium conditions of the mechanochemical route [1,4,31]. Thus, the rationale of preferring stoichiometric amount in the preparation of the powder blends is unavoidable formation of niobium borides in different stoichiometries.



Stoichiometric excess amount (25%) of boron source (B<sub>2</sub>O<sub>3</sub>) was representatively used in the milling experiments (5 h) along with stoichiometric amount in order to reveal the effect of reactant amount on the properties of mechanochemically synthesized products. Mechanical milling experiments were conducted by using a high-energy ball mill (Spex<sup>TM</sup> 8000 D Mixer/Mill) with a milling rate of 1200 r/min. Milling was performed with a ball-to-powder mass ratio (BPR) of 10:1 using hardened steel balls (diameter 6 mm) in a hardened steel vial (capacity 50 mL). Mechanical milling time is 1, 2, 3, 5, 7 and 9 h and as-blended (non-milled) powders were mixed and homogenized in a WAB<sup>TM</sup> T2C Turbula blender for 1 h. Sample handling was carried out in a glove box (Plaslabs<sup>TM</sup>) under purified Ar atmosphere in order to prevent interaction of particles with atmospheric conditions. In following milling experiments, selective HCl (Merck<sup>TM</sup> 37%) leaching was applied on the milled products in order to remove undesired MgO phase and other impurities released from the milling media. Leaching was carried out in a 4 mol/L HCl solution under the ultrasonic stirring (Bandelin<sup>TM</sup> Sonorex) for 15 min with a solid-to-liquid ratio of 1 g/10 cm<sup>3</sup>. Purified niobium boride powders (sample milled for 5 h after leaching with 4 mol/L HCl) were placed in an alumina boat and annealed in a tube furnace (Protherm<sup>TM</sup>) at 1500 °C for 4 h in flowing Ar atmosphere with a heating and cooling rate of 10 °C/min.

Thermodynamical data were theoretically calculated with the FactSage<sup>TM</sup> 6.2 thermochemical software. The phase compositions of the powders were performed by X-ray diffraction (XRD) technique using a D8 Advanced Series powder diffractometer (Bruker<sup>TM</sup>) with Cu K<sub>α</sub> (1.54060 Å) radiation with a step size of 0.02 ° at a rate of 2 (°)/min. International Center for Diffraction Data (ICDD) powder diffraction files were utilized in the identification of crystalline phases. The phase amounts in the milled and leached powder products were identified by the semi-quantitative Rietveld method. Thermal properties of the as-blended, milled and leached powders were examined by using a TA<sup>TM</sup> Instruments Q600 differential scanning calorimeter (DSC). DSC experiments were conducted in an alumina crucible up to a heating temperature of 1400 °C with a rate of 10 °C/min in Ar atmosphere. Fe impurities worn off from

the milling vial and balls were analyzed in the leach solution by Perkin Elmer<sup>TM</sup> 1100B atomic absorption spectrometer (AAS) and in the purified powders by vibrating sample magnetometer (VSM). Particle size measurements were conducted on the leached powders using a Microtrac<sup>TM</sup> Nano-flex particle size analyzer (PSA). In order to prevent agglomeration of the particles, powders were homogenized in a Bandelin Sonopuls<sup>TM</sup> ultrasonic homogenizer for 15 min using distilled water as aqueous media prior to particle size measurements. Microstructural characterizations of the powders were carried out by using a FEI-Quanta FEG 250 scanning electron microscope (SEM) coupled with an energy-dispersive X-ray spectrometer (EDX) and using a JEOL JEM-ARM200CFEG UHR transmission electron microscope (TEM).

### 3 Results and discussion

#### 3.1 Phase and thermal analyses of as-blended and milled powders

Figure 1 presents the XRD patterns of the as-blended Nb<sub>2</sub>O<sub>5</sub>-B<sub>2</sub>O<sub>3</sub>-Mg powders and those milled for different time. It is evident from Fig. 1 that there is no reaction after milling for 1 h since Nb<sub>2</sub>O<sub>5</sub> (ICDD card No.: 01-071-0336, Bravais lattice: primitive orthorhombic,  $a=0.617$  nm,  $b=2.917$  nm,  $c=0.393$  nm) and Mg (ICDD card No.: 35-0821, Bravais lattice: primitive hexagonal,  $a=b=0.329$  nm,  $c=0.521$  nm) phases are still present in the powder blend. No peaks belonging to the B<sub>2</sub>O<sub>3</sub> phase can be observed in the XRD patterns of the as-blended and 1 h of milled powders, which can be attributed to its amorphous nature. After milling for 2 h, the NbB (ICDD card No.: 32-0709, Bravais lattice: base-centered orthorhombic,  $a=0.330$  nm,  $b=0.872$  nm,  $c=0.317$  nm), NbB<sub>2</sub> (ICDD card No.: 35-0742, Bravais lattice: primitive hexagonal,  $a=b=0.311$  nm,  $c=0.327$  nm), Nb<sub>3</sub>B<sub>4</sub> (ICDD card No.: 03-065-2553, Bravais lattice: body-centred orthorhombic,  $a=0.330$  nm,  $b=1.408$  nm,  $c=0.314$  nm) and MgO (ICDD card No.: 01-079-0612, Bravais lattice: face-centred cubic,  $a=b=c=0.422$  nm) phases are observed in the microstructure. Besides, Nb<sub>2</sub>O<sub>5</sub> and Mg totally disappeared in the XRD patterns of the 2 h of milled powders. This indicates that a solid-state reaction takes place among the raw materials of Nb<sub>2</sub>O<sub>5</sub>, B<sub>2</sub>O<sub>3</sub> and Mg resulting in the niobium boride phases in three different compositions. Unlike the theoretical reduction reaction given in Eq. (1) which yields the NbB<sub>2</sub> phase as a main reaction product, NbB<sub>2</sub> is not the dominant phase in the microstructure of the milled powders. The occurrence of niobium borides in different stoichiometries is expected. The absence of dominance in the NbB<sub>2</sub> phase can be attributed to the proposed Nb-B binary phase diagrams,

in which NbB ( $T_m \sim 2800$  °C, 50% Nb, mole fraction), Nb<sub>3</sub>B<sub>4</sub> ( $T_m \sim 2900$  °C, 43% Nb) and NbB<sub>2</sub> ( $T_m \sim 3000$  °C, 25–35% Nb) phases were defined as stable compounds having very close melting points and homogeneity ranges [1,4,5].

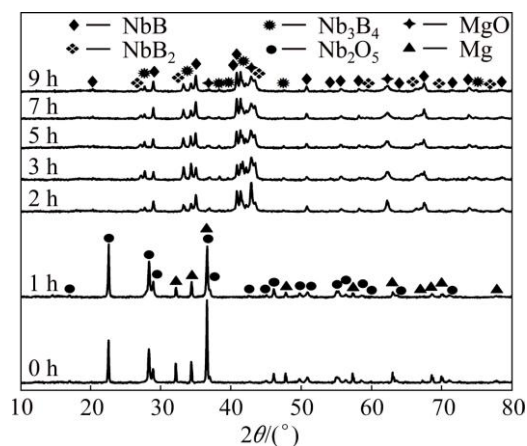


Fig. 1 XRD patterns of as-blended Nb<sub>2</sub>O<sub>5</sub>-B<sub>2</sub>O<sub>3</sub>-Mg powders and those milled for different time

It is also understandable that products of the actual reaction triggered by the mechanical milling which are away from the equilibrium conditions may not completely conform to those of the ideal case. Since mechanochemical synthesis process is a kind of mechanical alloying induced by redox/reduction reactions, the formation of products is favorable at the contact points of the particles during repeated collisions. Once NbB, Nb<sub>3</sub>B<sub>4</sub> and NbB<sub>2</sub> phases formed in the sequence of requiring lower amount of boron after milling for 2 h, this variety in stoichiometry did not change. It was reported that single-phase niobium boride could not be obtained via combustion synthesis of elemental powder compacts even though specific ratios of elemental Nb to B were used as the initial compositions according to the Nb-B binary phase diagram [24]. The variety in the stoichiometry of niobium borides can be attributed to some kinetic factors and the nonequilibrium conditions of mechanochemical and combustion synthesis processes [31]. Studies in the current literature showed that the single phase of niobium borides (without any remaining Nb or B) could be achieved by applying high or low temperature processes under steady-state conditions [13,15,19,22,23]. Moreover, the formation of niobium borides with major NbB and minor NbB<sub>2</sub> and Nb<sub>3</sub>B<sub>4</sub> phases by mechanochemistry of oxide raw materials at room temperature may be different from some other studies which used elemental starting materials and indicated the NbB<sub>2</sub> as the dominant boride phase [28,29]. Due to the fact that mechanochemical synthesis is a room temperature method without applying any external heat,

the formed NbB, Nb<sub>3</sub>B<sub>4</sub> and NbB<sub>2</sub> phases keep their presence in the powders and have no chance to transform to a single-phase form after the reaction took place at 2 h of milling.

Although niobium borides were achieved after milling for 2 h, milling was extended up to 9 h in order to detect any probable degradation of the current reaction products and any formation of a new phase. According to the XRD patterns in Fig. 1, there is an observable broadening in the intensities of the niobium boride and MgO phases by extending milling time up to 9 h, which represents a decrease in their crystallite size. On the other hand, there are no remaining elemental Nb or B and no additional compounds between Nb–Mg, B–Mg, Nb–Mg–O, Nb–B–O, B–Mg–O in the detection limit of XRD. IIZUMI et al [28] reported the mechanical alloying of Nb and B mixtures and stated that NbB<sub>2</sub> was obtained after 20 h of milling but unreacted Nb and B still remained in the structure. Only after prolonging the milling time to 50 h, the XRD peaks of the Nb phase disappeared and a single phase of NbB<sub>2</sub> was obtained in their investigation [28]. However, it should be stated that their process is not an economically feasible way to produce niobium boride powders since it requires high energy consumption due to the very long milling time and high cost of elemental starting materials. In this case, only replacement reaction was induced by mechanical milling of the Nb and B powder particles [28]. In the present investigation, however, both reduction and replacement reactions took place by using Nb<sub>2</sub>O<sub>5</sub> and B<sub>2</sub>O<sub>3</sub> with the presence of Mg which initiated the spontaneous ignition between the particles without any external applied heat and hence shortened the overall reaction time. Actually, the impact energy obtained with the collision of the milling balls, milling walls and powder particles results in a repeated fracture, friction and welding mechanism during the process [31–35]. This mechanical energy accumulates in the system, heat conductivity of the milling medium provides the formation of hot spots and mechanical energy converts into chemical energy which proceeds the synthesis process by an explosive reaction [31–35]. Large amount of heat is released at the time of the explosive and intensive exothermic reaction which proceeds spontaneously and provides the reduction of the reactants until whole Mg converts into MgO. This phenomenon could increase the possibility of yielding products in different stoichiometry. Thus, the products of this highly exothermic reaction are not the same with the theoretical one in Eq. (1) which is based on the equilibrium conditions.

On the basis of the Nb–B binary phase diagram, it can be thought that the phases with low boron contents like NbB and Nb<sub>3</sub>B<sub>4</sub> emerged due to the insufficient

amounts of boron source. Therefore, the stoichiometric excess amount of B<sub>2</sub>O<sub>3</sub> (25%) was representatively used during milling experiments (5 h) in order to observe probable changes in the composition of the powders. Figure 2 shows the XRD patterns of the Nb<sub>2</sub>O<sub>5</sub>–B<sub>2</sub>O<sub>3</sub>–Mg powders milled for 5 h with excess of 25% B<sub>2</sub>O<sub>3</sub>. As seen from Fig. 2 that Nb<sub>3</sub>B<sub>4</sub> emerged as a dominant phase in the presence of NbB<sub>2</sub>, NbB and MgO phases in the microstructure. The utilization of stoichiometric excess amount of B<sub>2</sub>O<sub>3</sub> provides complete reduction process and results in an increase in the intensities of Nb<sub>3</sub>B<sub>4</sub> peaks and decrease in the NbB peaks, indicating an increase in the amount of niobium borides with high boron content. Excess usage of boron source did not change the types of the formed niobium boride phases but it changed their amount. Thus, increasing the amount of boron source in the overall powder blend still yielded the formation of a multi-phase powder. Thus, only stoichiometric amount of the reactants was used in the following experiments, since the excess amount of boron source does not affect the multi-phase feature of the milled powders.

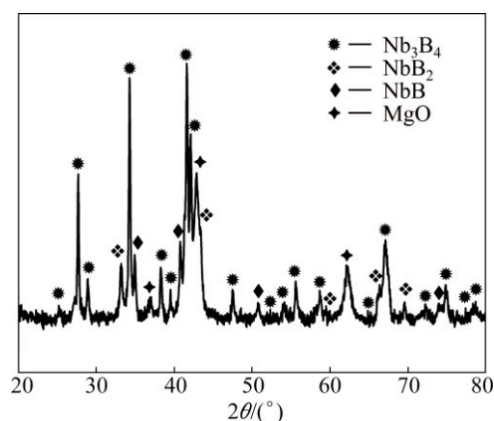
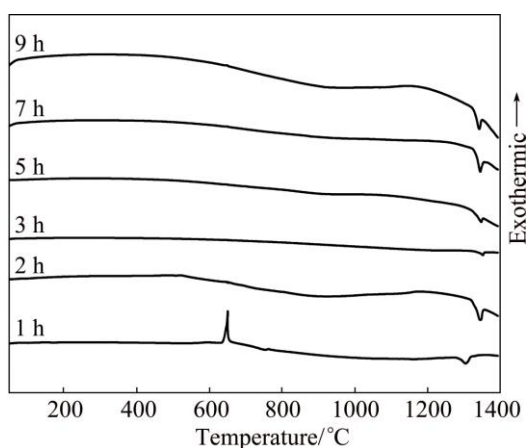


Fig. 2 XRD patterns of Nb<sub>2</sub>O<sub>5</sub>–B<sub>2</sub>O<sub>3</sub>–Mg powders milled for 5 h with excess of 25% B<sub>2</sub>O<sub>3</sub>

In order to determine thermal behavior of the Nb<sub>2</sub>O<sub>5</sub>–B<sub>2</sub>O<sub>3</sub>–Mg powder blends, DSC analyses were conducted on the milled (1, 2, 3, 5, 7 and 9 h) samples (Fig. 3). The DSC scan of the powders milled for 1 h shows a sharp exotherm peak at about 650 °C, a small narrow exotherm peak at about 760 °C and a small broad endotherm peak at about 1300 °C. Although 1 h milled powders contain Nb<sub>2</sub>O<sub>5</sub>, B<sub>2</sub>O<sub>3</sub> and Mg phases (Fig. 1), endothermic peaks corresponding to the melting of B<sub>2</sub>O<sub>3</sub> at 450 °C, the melting of Mg at 650 °C and the boiling of residual Mg at 1090 °C cannot be detected from the DSC scans. The sharp exothermic peak at about 650 °C emerges as a result of Nb<sub>2</sub>O<sub>5</sub> reduction by Mg and Mg oxidation. In other words, Mg was considerably oxidized to form MgO at 650 °C before reaching its melting and boiling points. Consequently, elemental Nb phase formed

due to this instantaneous oxidation/reduction phenomenon. Moreover, the small narrow exotherm peak at about 760 °C corresponds to the formation of B particles subsequent to the oxidation of Mg. It can be said that a replacement reaction between  $B_2O_3$  and Mg takes place and it enables free B particles to occur, which afterwards participate into the boride formation. This exothermic behavior emerged from the magnesiothermic reduction of  $B_2O_3$  was also reported at ~800 °C in the DTA experiments of Mg– $B_2O_3$ –Nb–C and Mg– $B_2O_3$ –Nb systems [29,30]. Moreover, the proposed reactions' sequence in this study is consistent with the thermodynamic evaluation. The free energies of the formation of Nb (originated from the reduction of  $Nb_2O_5$  by Mg) and B (originated from the reduction of  $B_2O_3$  by Mg) were calculated as  $\Delta G_{298}^\ominus = -1090$  and  $-515$  kJ, respectively. Thus, the small broad endothermic peak at about 1300 °C corresponds to the formation of Nb boride phases due to reactions between Nb and B particles. On the other hand, DSC scans of the 2, 3, 5, 7 and 9 h of milled powders (Fig. 3) do not have any exothermic and endothermic peaks corresponding to the formation of MgO, Nb and B phases because they already comprise NbB,  $NbB_2$ ,  $Nb_3B_4$  and MgO phases after mechanochemical synthesis (Fig. 1). 2 h of milled powders show an endotherm peak having an onset temperature at about 1305 °C and a maximum peak point at about 1345 °C. The onset temperature of this endotherm peak almost intersects the endothermic peaking point of the powders milled for 1 h. Thus, it can be attributed to the overlapped peak of Nb boride formation originated from remaining Nb which is under the detection limit of XRD (<2%) and to the transformation of Nb boride phases. The peak overlapping is understandable because the reaction took place after 2 h and the whole amount of reduced Nb may not contribute to the boride formation. When milling time increased to 3 h, the endothermic peak became



**Fig. 3** DSC scans of  $Nb_2O_5$ – $B_2O_3$ –Mg powders milled for different time

smaller and narrower than that of 2 h milled powders and its peak point shifted to 1370 °C, which only indicates the phase transformation of Nb borides. This implies the completion of the boride formation reaction with no evidence of unreacted Nb. As milling time prolonged up to 9 h, the endothermic peak transformed into a sharper peak than those milled for shorter time without changing its maximum temperature point due to the smaller-sized NbB,  $NbB_2$  and  $Nb_3B_4$  particles having more reactive surfaces than those milled for shorter time.

### 3.2 Phase, chemical and thermal analyses of milled and leached powders

Figure 4 shows the XRD patterns of the  $Nb_2O_5$ – $B_2O_3$ –Mg powders milled for 2, 3, 5, 7 and 9 h after leaching. Figure 4 reveals that the unwanted by-product MgO was completely removed from the powder blend after leaching with 4 mol/L HCl and pure niobium boride powders comprising NbB,  $NbB_2$  and  $Nb_3B_4$  phases were obtained. As seen from the XRD patterns of the leached samples, there is no residual magnesium chloride, oxychloride or hydroxychloride as leaching products which indicates the effectiveness of the leaching parameters. The dissolution of MgO was also confirmed by AAS analyses of the leach solutions decanted from the residual powders. The amount of Mg in the leach solution increases from  $5337 \times 10^{-6}$  to  $8312 \times 10^{-6}$  (mass fraction), as the milling time increases from 3 to 9 h. This shows that the dissolution of MgO in HCl was enhanced with increasing milling time. This phenomenon can be attributed to the higher surface areas of the particles milled for longer time [31].

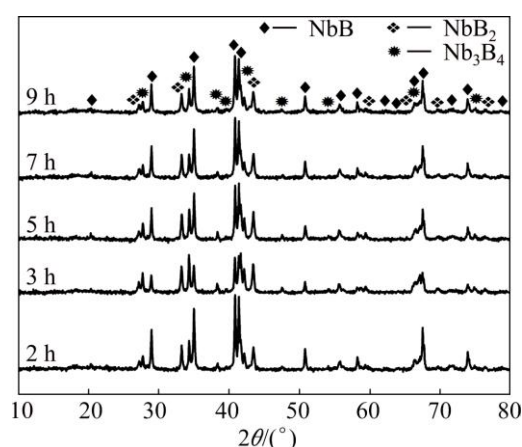


**Fig. 4** XRD patterns of  $Nb_2O_5$ – $B_2O_3$ –Mg powders milled for different time after leaching

Furthermore, AAS analyses of the leach solution showed that it consists of  $35 \times 10^{-6}$  Fe for the powders after milling for 5 h and leaching with 4 mol/L HCl. The remaining Fe impurity in the powders can also be determined from the magnetic measurements, which

provided that the material has a ferromagnetic tendency. Figures 5(a) and (b) exhibit the room-temperature magnetic field versus magnetization curves of the  $\text{Nb}_2\text{O}_5\text{-B}_2\text{O}_3\text{-Mg}$  powder milled for 5 h before and after leaching with 4 mol/L HCl. The powders milled for 5 h are paramagnetic (Fig. 5(a)), which points out the presence of Fe impurity in the order of  $10^{-6}$ . As seen from Fig. 5(b), the mechanochemically synthesized niobium boride powders ( $\text{NbB-NbB}_2\text{-Nb}_3\text{B}_4$ ) became diamagnetic after leaching treatment which definitely proves the absence of Fe in the resultant powders. Both the AAS analysis and magnetic measurements indicate that Fe impurity released from the milling media is completely removed by HCl leaching as well as MgO.

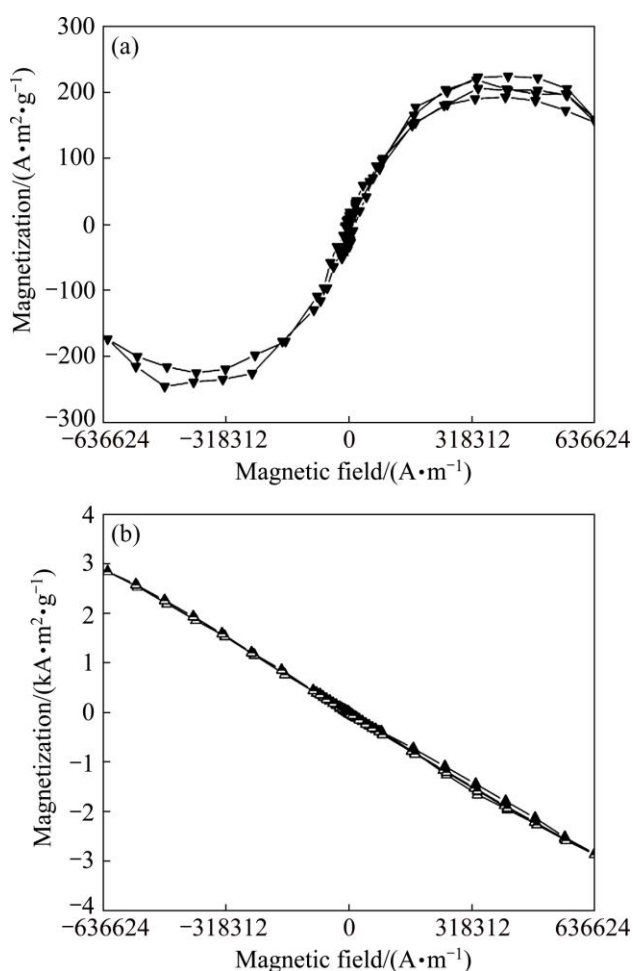


**Fig. 5** Room-temperature magnetic measurement of  $\text{Nb}_2\text{O}_5\text{-B}_2\text{O}_3\text{-Mg}$  powders milled for 5 h before (a) and after (b) leaching with 4 mol/L HCl

Table 1 exhibits the semi-quantitative phase analyses of the milled (for different time) and leached powders. Analysis results were obtained from the Rietveld refinement method based on the XRD patterns in Fig. 4. Rietveld refinement method was conducted on the milled and leached powders for the determination of the estimated amount of the niobium boride phases

eliminated from the MgO contamination. As seen from Table 1, extending milling time up to 9 h seems to change the compositions of the leached products. The amounts of NbB,  $\text{NbB}_2$  and  $\text{Nb}_3\text{B}_4$  phases differ from one another at each milled powder. After reduction reaction took place at the end of milling for 2 h, NbB emerged with 55% (volume fraction) dominant phase. However,  $\text{Nb}_3\text{B}_4$  occurred with 43.3% (volume fraction) major phase at the end of milling for 3 h. Besides, the amounts of  $\text{NbB}_2$  and  $\text{Nb}_3\text{B}_4$  phases gradually decreased and NbB phase had the majority in the total volume with increasing milling time from 3 to 9 h. The change of dominant phase in the 2 and 3 h milled powders arose from the incidental conditions of the mechanochemical synthesis process such as interaction of reactant particles on  $\text{B}_2\text{O}_3$ -poor or  $\text{B}_2\text{O}_3$ -rich surfaces until a homogeneous distribution was reached. Thus, it can be said that a steady-state condition in the overall reaction could be achieved at milling time over 3 h, at which a consistency in the major phase was obtained. These findings are also in good agreement with the XRD and DSC analyses in Figs. 1, 3 and 4. Thus, NbB is the dominant phase after milling for 5, 7 and 9 h and subsequent leaching.

**Table 1** Semi-quantitative phase analyses of milled and leached powders, obtained from Rietveld refinement method based on their XRD patterns

Milling time/h	$\varphi(\text{NbB})/\%$	$\varphi(\text{NbB}_2)/\%$	$\varphi(\text{Nb}_3\text{B}_4)/\%$
2	55.0	15.9	29.1
3	29.8	26.9	43.3
5	43.2	22.1	34.7
7	52.2	21.4	26.4
9	55.0	19.4	25.6

Figure 6 presents the DSC scans of the  $\text{Nb}_2\text{O}_5\text{-B}_2\text{O}_3\text{-Mg}$  powders after milling for 5 and 9 h and leaching with 4 mol/L HCl. They almost show the same tendency up to 1300 °C. DSC scans of the milled and leached powders given in Fig. 6 do not show any sharp exothermic peak. This is the solid evidence of sufficient purity that milled powders achieved after leaching with 4 mol/L HCl. Even if a small amount of MgO (which cannot be detected by XRD) was still present in the leached powders, it would react with niobium boride phases to form  $\text{Mg}_x\text{Nb}_y\text{O}_z$  compound during the heating up to 1300 °C, which is a highly exothermic reaction. On the basis of XRD, AAS, DSC analyses and magnetic measurements of the milled powders after leaching treatment, it is clear that the resultant powders do not include any contamination or other unwanted reaction products. Furthermore, DSC scans in Fig. 6 show decrease in heat flow at temperatures higher than 1200 °C.

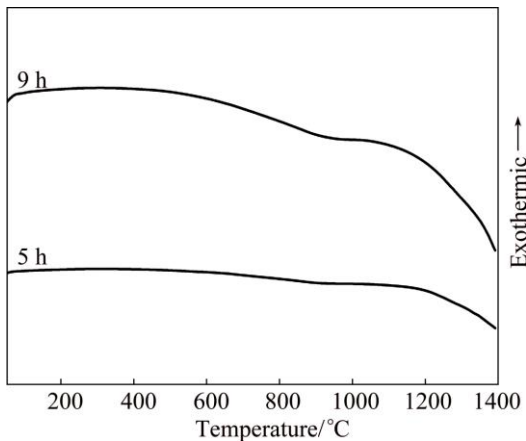


**Fig. 6** DSC scans of  $\text{Nb}_2\text{O}_5\text{-B}_2\text{O}_3\text{-Mg}$  powders milled for 5 and 9 h after leaching

### 3.3 Phase analysis of annealed powders

In order to determine the reason of the heat flow decrease almost starting from 1200 °C, milled and leached powders were annealed at 1500 °C for 4 h which is over the heating capability of the calorimeter. Figure 7 shows the XRD pattern of the milled  $\text{Nb}_2\text{O}_5\text{-B}_2\text{O}_3\text{-Mg}$  powders for 5 h after leaching with 4 mol/L HCl and annealing at 1500 °C for 4 h. Figure 7 clearly shows that after annealing process, NbB, NbB<sub>2</sub> and Nb<sub>3</sub>B<sub>4</sub> containing powders completely transform to the NbB phase which was already dominant in the microstructure after leaching treatment (Table 1). Thus, the sharp decrease in the heat flow corresponds to the NbB phase transformation at high temperature. On the other hand, the microstructure of the 3 h milled and leached powders (Fig. 4) remain the same after annealing at 1500 °C, which presents niobium boride phases with different compositions. This indicates that 3 h milling does not provide sufficient energy for the complete transformation of niobium boride phases during annealing. It has been already reported that mechanical milling changes the homogeneity and reactivity of powder particles [31]. Activation energy absorbed by the particles during milling assisted the phase transformation of the niobium borides. The absorbed activation energy after 3 h milling is not adequate for the reaching of the energy barrier towards the complete transformation whereas enough activation energy produced after 5 h triggering the complete phase transformation during heat treatment [31,35]. Since NbB, NbB<sub>2</sub> and Nb<sub>3</sub>B<sub>4</sub> phases are all very stable niobium boride phases with close melting points (2800–3000 °C) according to the Nb–B phase diagram, the phase change mechanism can also be explained by isothermal annealing condition of highly activated boride powders during 4 h of holding time [1,4]. This is well known that the mechanical activation of the powder particles and subsequent annealing enables the

activated particles to react at lower temperatures than thermodynamically required [31]. Thus, a deformation-induced NbB single phase could only be obtained after milling for 5 h and subsequent annealing (Fig. 7). This might be the result of the reaction between niobium boride phases with low Nb contents (Nb<sub>3</sub>B<sub>4</sub>, NbB<sub>2</sub>) to yield NbB phase with high Nb content releasing small amount of B. However, the diffraction peaks of B cannot be detected by XRD analysis due to its probable incorporation of small B atoms into orthorhombic NbB structure.

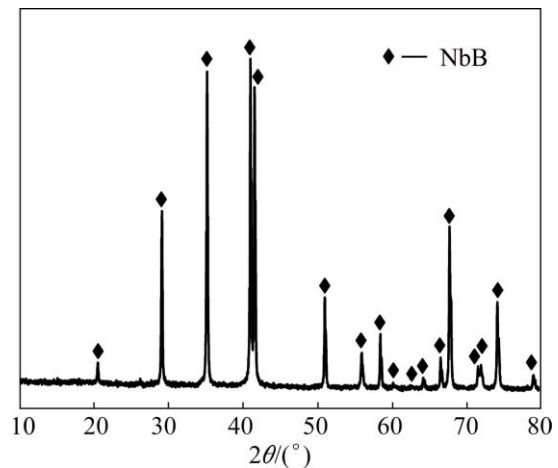
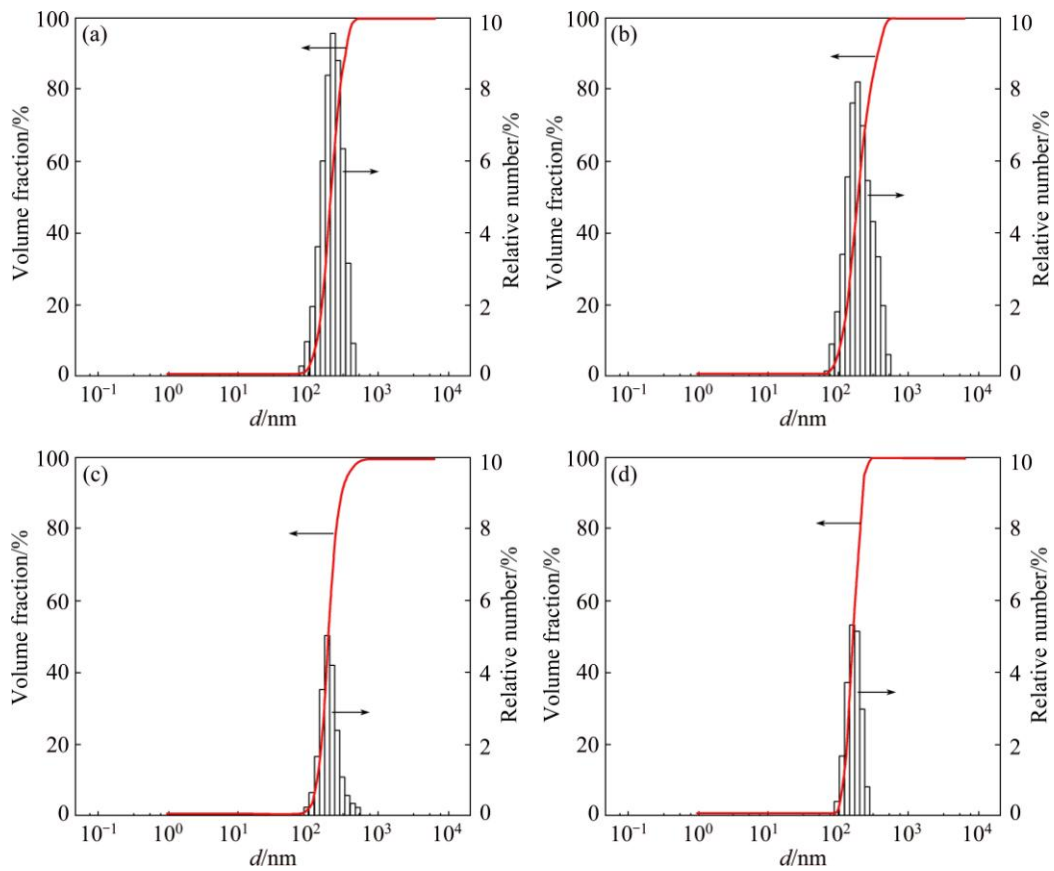


**Fig. 7** XRD pattern of  $\text{Nb}_2\text{O}_5\text{-B}_2\text{O}_3\text{-Mg}$  powders milled for 5 h after leaching and annealing at 1500 °C

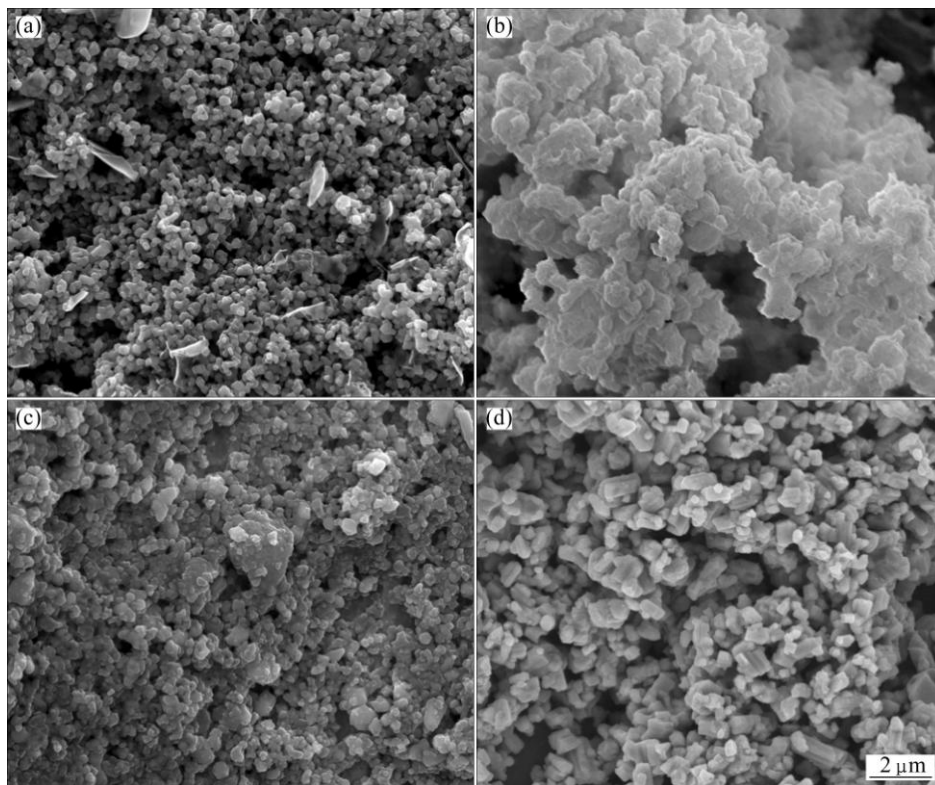
### 3.4 Particle size and microstructural analyses of as-blended, milled, leached and annealed powders

Figure 8 shows the particle size distributions of the milled powders after leaching with 4 mol/L HCl. Figures 8(a)–(d) display the average sizes of the leached particles as about 219, 194, 197 and 166 nm for the powders milled for 3, 5, 7 and 9 h after leaching, respectively. The  $\text{Nb}_2\text{O}_5\text{-B}_2\text{O}_3\text{-Mg}$  powder blends milled for 3 h resulted in a significant decrease in the particle size from micro- to nano-scales, even after the leaching process. Additional milling of 6 h reduces the particle size from 219 to 166 nm in the resultant powders. The results of the particle sizes for the milled and leached powders show that high energy ball milling is an effective way to obtain small particles from large starting materials.

Figure 9 shows the secondary electron SEM images of the as-blended  $\text{Nb}_2\text{O}_5\text{-B}_2\text{O}_3\text{-Mg}$  powders, those milled for 5 h and those leached with 4 mol/L HCl and those annealed at 1500 °C. As seen from Fig. 9(a), as-blended powders have irregular agglomerates and spherical and leaf-like particles. Figure 9(b) reveals that microstructure of the powders milled for 5 h involves spherical-shaped niobium boride particles embedded in blurred MgO particles, which is in agreement with the XRD patterns in Fig. 1. Figure 9(b) clearly shows the



**Fig. 8** Particle size distributions of  $\text{Nb}_2\text{O}_5\text{-B}_2\text{O}_3\text{-Mg}$  powders milled for different time after leaching: (a) 3 h; (b) 5 h; (c) 7 h; (d) 9 h



**Fig. 9** SEM images of as-blended  $\text{Nb}_2\text{O}_5\text{-B}_2\text{O}_3\text{-Mg}$  powders and those after milling, leaching and annealing processes: (a) As-blended powders (0 h); (b) Powders milled for 5 h; (c) Powders milled for 5 h after leaching; (d) Powders milled for 5 h after leaching and annealing at 1500 °C

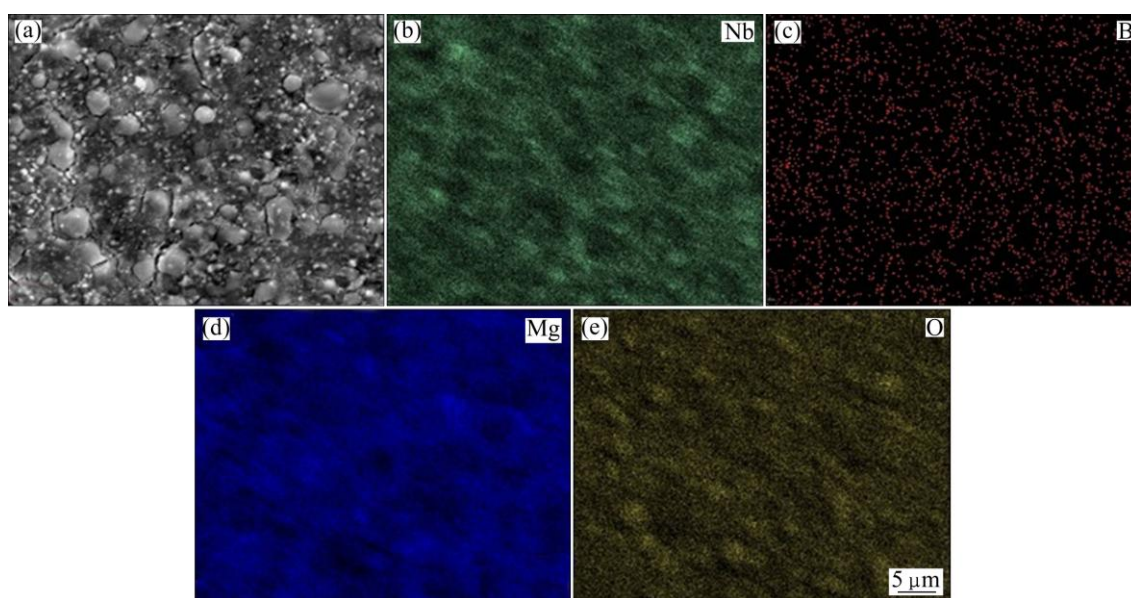
adherence and agglomeration of the particles due to the heat released by the mechanochemical reaction. The microstructure of the powders after milling for 5 h and subsequent leaching given in Fig. 9(c) exhibits a homogenous particle distribution and consists of equiaxed particles smaller than 700 nm in the absence of the MgO phase with blurred microstructure. However, agglomeration of the powder particles prevents the observation of the smaller ones. Therefore, particle size measurement carried out after homogenization of the powder blends gives more accurate results of about 190 nm, as previously presented in Fig. 8(b). Figure 9(d) shows the microstructure of the powders milled for 5 h after leaching with 4 mol/L HCl and annealing at 1500 °C for 4 h, indicating the effect of heat treatment and hence phase transformation (from niobium borides comprising NbB, NbB<sub>2</sub> and Nb<sub>3</sub>B<sub>4</sub> phases to the single phase NbB) on the morphologies of the particles. It can be seen from Fig. 9(d) that annealed powders consist of distinct particles with relatively clear boundaries which are larger than those of the milled and leached ones (Fig. 9(c)).

In order to reveal the phase distribution clearly, SEM/EDX analyses were carried out on compacted pellets of the powders. Figure 10 shows the SEM/EDX analyses of the pellet obtained from the compaction of the Nb<sub>2</sub>O<sub>5</sub>–B<sub>2</sub>O<sub>3</sub>–Mg powders milled for 5 h. Figures 10(b)–(e) present the associated elemental maps for Nb, B, Mg and O taken from the pellet of the 5 h-milled powders. The weak signals of B particles shown in Fig. 10(c) can be associated with the suppression effect of the other strong signals of the elements (Nb, Mg and O). The elemental Mg map (Fig. 10(d)) coincides almost

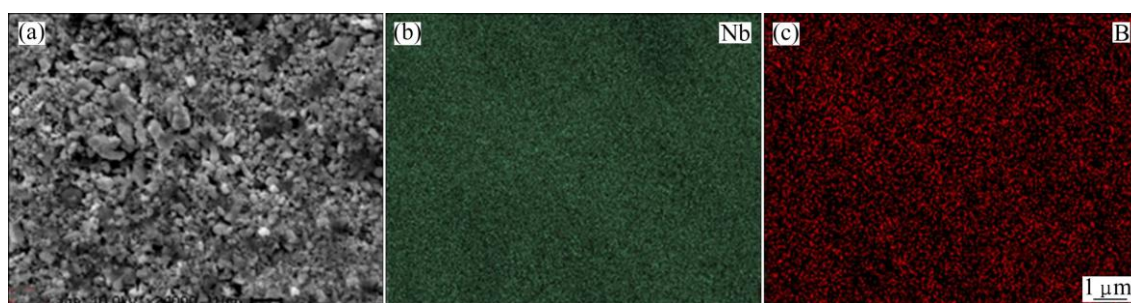
entirely with the elemental O map (Fig. 10(e)), suggesting the presence of the MgO phase. SEM/EDX analyses of the Nb<sub>2</sub>O<sub>5</sub>–B<sub>2</sub>O<sub>3</sub>–Mg powders milled for 5 h confirm the phase analyses obtained by XRD (Fig. 1). Furthermore, the distribution of the Nb, B, Mg and O elements throughout the microstructure reveals the adherence and simultaneous existence of niobium boride and MgO phases, which is also in good agreement with the blurred morphology of the milled powders given in Fig. 9(b).

Figure 11 shows the SEM/EDX analyses of the pellet obtained from the compaction of the Nb<sub>2</sub>O<sub>5</sub>–B<sub>2</sub>O<sub>3</sub>–Mg powders milled for 5 h after leaching. Figure 11 presents the secondary electron SEM image and the associated elemental maps for Nb and B taken from the pellet of the 5 h-milled powders after leaching. The elemental Nb map (Fig. 11(b)) coincides almost entirely with the elemental B map (Fig. 11(c)), suggesting the presence of niobium boride phase. Furthermore, comparing Figs. 10(b) and (c) with Figs. 11(b) and (c), it is clear that the signals arising from Nb and B elements considerably increase after leaching. Besides, any signals of Mg and O were not detected during SEM/EDX analyses of the leached powders. This is the result of the removal of unwanted MgO phase (Fig. 4) after leaching, which also proves the purity of the niobium boride powders.

Figure 12 shows the TEM images of the Nb<sub>2</sub>O<sub>5</sub>–B<sub>2</sub>O<sub>3</sub>–Mg powders milled for 5 h after leaching with 4 mol/L HCl. Figure 12(a) shows a bright-field (BF) image of an equiaxed particle approximately 200 nm in size, which is consistent with the reported average particle size of the leached powders shown in Fig. 8(b).



**Fig. 10** SEM image (a) of pellet obtained from compaction of Nb<sub>2</sub>O<sub>5</sub>–B<sub>2</sub>O<sub>3</sub>–Mg powders milled for 5 h and corresponding elemental maps for Nb (b), B (c), Mg (d) and O (e)



**Fig. 11** SEM image (a) of pellet obtained from compaction of  $\text{Nb}_2\text{O}_5\text{-B}_2\text{O}_3\text{-Mg}$  powders milled for 5 h after leaching and corresponding elemental maps for Nb (b) and B (c)

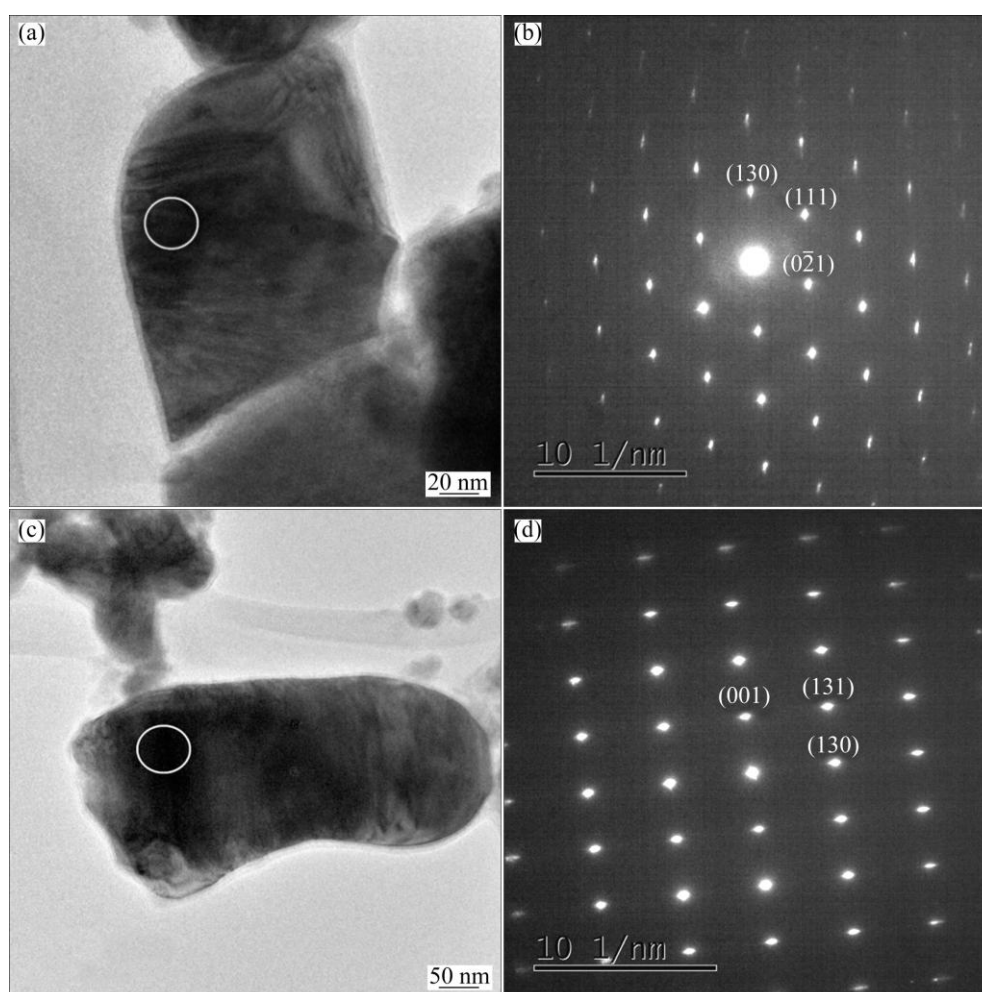


**Fig. 12** TEM images of  $\text{Nb}_2\text{O}_5\text{-B}_2\text{O}_3\text{-Mg}$  powders milled for 5 h after leaching: (a) Bright-field (BF) image; (b) Corresponding selected area diffraction pattern (SADP) revealing the presence of NbB phase (Camera length is 80 cm and zone axis is  $[\bar{3}12]$ ); (c) Bright-field (BF) image; (d) Corresponding selected area diffraction pattern (SADP) revealing the presence of NbB phase (Camera length is 80 cm and zone axis is  $[3\bar{1}0]$ )

Selected area diffraction pattern (SADP) taken from this particle in Fig. 12(b) is a spot pattern which reveals the presence of the orthorhombic NbB phase from a single grain (Camera length is 80 cm and zone axis is  $[\bar{3}12]$ ). Figure 12(c) shows a bright-field (BF) image of an ellipsoid particle approximately 600 nm in size, which represents larger particles in the obtained powders.

Selected area diffraction pattern (SADP) taken from this particle in Fig. 12(d) is a spot pattern which also reveals the presence of the orthorhombic NbB phase from a single grain (Camera length is 80 cm and zone axis is  $[3\bar{1}0]$ ). NbB was also detected as the dominant phase in the XRD pattern in Fig. 4 and semi-quantitative phase analysis in Table 1 of the powders milled for 5 h after

leaching. Additional TEM characterizations carried out on other grains revealed spot patterns of single crystalline particles with different zone axes, which belong to the NbB phase.

Overall, considering its simplicity and advantages of the processing route and the low costs of the raw materials, it is expected that this study would become an inspiration for new investigations in the powder metallurgical synthesis of some other materials. Further, fine and homogeneous microstructure of the products obtained in the mechanochemical process can be an attractive precursor for the bulk borides or boride-based composites. Following studies will be intended to investigate the sintering behaviours of the obtained niobium boride powders and to reveal the advantage and use of the multi-phase boride products.

## 4 Conclusions

1) Niobium boride and MgO phases were achieved after 2 h of milling in a high energy ball mill using Nb<sub>2</sub>O<sub>5</sub>, B<sub>2</sub>O<sub>3</sub> and Mg powder blends. There were no remaining elemental Nb or B and no additional compounds between Nb–Mg, B–Mg, Nb–Mg–O, B–Mg–O, in the detection limit of XRD. DSC scans of the milled powders did not have any exothermic and endothermic peaks corresponding to the formation of MgO, Nb and B phases because they included niobium boride and MgO phases after mechanochemical synthesis.

2) Subsequent leaching with 4 mol/L HCl removed the unwanted MgO phase and obtained pure NbB–NbB<sub>2</sub>–Nb<sub>3</sub>B<sub>4</sub> powders. Fe impurity released from the milling media could be completely removed by HCl leaching as well as MgO. The purity of the niobium boride powders were confirmed by AAS and DSC analyses and magnetic measurements. Furthermore, extending milling time up to 9 h changed the compositions of the final products after leaching, i.e., the amount of NbB, NbB<sub>2</sub> and Nb<sub>3</sub>B<sub>4</sub> phases.

3) Single phase NbB powders were achieved by annealing of the purified powders (after milling for 5 h and subsequent leaching) at 1500 °C for 4 h.

4) The removal of MgO and the formation of niobium boride phases after milling and leaching were also supported by SEM/EDX analyses. Orthorhombic NbB phase was also identified by TEM. Resultant niobium boride powders had an average particle size of ~200 nm which was proved both by particle size measurements and BF image monitored by TEM analysis.

5) A novel and simple powder metallurgy method was achieved to fabricate nano-sized niobium boride powders in high-purity through an economical way from

their oxide raw materials in the presence of a strong reducing agent.

## Acknowledgements

This research was financially supported by “The Scientific and Technological Research Council of Turkey (TÜBİTAK)” with the project title of “Synthesis of Refractory Metal Borides via Three Different Production Methods from Solid, Liquid and Gas Raw Materials for Various Application Areas; Sintering, Characterization, Comparison of Process and Final Products” and with the project number of 112M470. Further, the authors wish to express their appreciations to Dr. Mehmet Ali Gülgün for his help with the TEM investigations and Dr. Orhan Kamer for his help in magnetic measurements.

## References

- [1] MASSALSKI T B. Binary alloy phase diagrams [M]. 2nd ed. Materials Park, OH: ASM International, 1990.
- [2] IVANOVSKY A L, MEDVEDEVA N I, MEDVEDEVA J E. Quantum-chemical analysis of the chemical stability and cohesive properties of hexagonal TiB<sub>2</sub>, VB<sub>2</sub>, ZrB<sub>2</sub> and NbB<sub>2</sub> [J]. Mendeleev Communications, 1998, 8(4): 129–131.
- [3] TSUCHIDA T, KAKUTA T. Synthesis of NbC and NbB<sub>2</sub> by MA-SHS in air process [J]. Journal of Alloys and Compounds, 2005, 398: 67–73.
- [4] RUDY E, WINDISCH S. Ternary phase equilibria in transition metal boroncarbonesilicon systems [M]. OH: Wright-Patterson Air Force Base, 1966.
- [5] OKAMOTO H. B–Nb (boron–niobium) [J]. Journal of Phase Equilibria and Diffusion, 2008, 29(6): 539.
- [6] JUNIOR L A B, COELHO G C, NUNES C A, SUZUKI P A. New data on phase equilibria in the Nb-rich region of the Nb–B system [J]. Journal of Phase Equilibria, 2003, 24(2): 140–146.
- [7] PEÇANHA R M. Thermodynamic modeling of the Nb–B system [J]. Intermetallics, 2007, 15: 999–1005.
- [8] YAMAMOTO A, TAKAO C, MASUI T, IZUMI M, TAJIMA S. High-pressure synthesis of superconducting Nb<sub>1-x</sub>B<sub>2</sub> (x=0–0.48) with the maximum T<sub>c</sub>=9.2 K [J]. Physica C, 2002, 383: 197–206.
- [9] JOSEPH P J T, SINGH P P. Theoretical study of electronic structure and superconductivity in Nb<sub>1-x</sub>B<sub>2</sub> alloys [J]. Physica C, 2003, 391: 125–130.
- [10] TAKEYA H, MATSUMOTO A, HIRATA K, SUNG Y S, TOGANO K. Superconducting phase in niobium diborides prepared by combustion synthesis [J]. Physica C, 2004, 412–414: 111–114.
- [11] MUDGEL M, AWANA V P S, BHALLA G L, KISHAN H. Superconductivity of non-stoichiometric intermetallic compound NbB<sub>2</sub> [J]. Solid State Communications, 2008, 147: 439–442.
- [12] REN Z A, KUROIWA S, TOMITA Y, AKIMITSU J. Structural phase evolution and superconductivity in the non-stoichiometric intermetallic compound niobium diboride [J]. Physica C, 2008, 468: 411–416.
- [13] MOTOJIMA S, SUGIYAMA K, TAKAHASHI Y. Chemical vapor deposition of niobium diboride (NbB<sub>2</sub>) [J]. Journal of Crystal Growth, 1975, 30: 233–239.
- [14] PESHEV P, LEYAROVSKA L, BLIZNAKOV G. On the borothermic preparation of some vanadium, niobium and tantalum borides [J]. Journal of the Less Common Metals, 1968, 15: 259–267.
- [15] MATSUDAIRA T, ITOH H, NAKA S. Synthesis of niobium boride powder by solid-state reaction between niobium and amorphous

- boron [J]. *Journal of the Less Common Metals*, 1989, 155(2): 207–214.
- [16] JUNIOR L A B, COELHO G C, NUNES C A, SUZUKI P A. New data on phase equilibria in the Nb-rich region of the Nb–B system [J]. *Journal of Phase Equilibria*, 2003, 24(2): 140–146.
- [17] TAKAHASHI T, KAWAMATA S, NOGUCHI S, ISHIDA T. Superconductivity and crystal growth of NbB<sub>2</sub> [J]. *Physica C*, 2005, 426–431: 478–481.
- [18] NUNES C A, KACZOROWSKI D, ROGL P, BALDISSERA M R, SUZUKI P A, COELHO G C, GRYSTIV A, ANDRE G, BOUREE F, OKADA S. The NbB<sub>2</sub>-phase revisited: Homogeneity range, defect structure, superconductivity [J]. *Acta Materialia*, 2005, 53: 3679–3687.
- [19] JHA M, RAMANUJACHARY K V, LOFLAND S E, GUPTA G, GANGULI A K. Novel borothermal process for the synthesis of nanocrystalline oxides and borides of niobium [J]. *Dalton Transactions*, 2011, 40: 7879–7888.
- [20] CHENG Y, CHOI S, WATANABE T. Synthesis of niobium boride nanoparticle by RF thermal plasma [J]. *Journal of Physics: Conference Series*, 2013, 441: 012031-1–6.
- [21] MAEDA H, YOSHIKAWA T, KUSAKABE K, MOROOKA S. Synthesis of ultrafine NbB<sub>2</sub> powder by rapid carbothermal reduction in a vertical tubular reactor [J]. *Journal of Alloys and Compounds*, 1994, 215: 127–134.
- [22] CAI P, YANG Z, SHI L, CHEN L, ZHAO A, GU Y, QIAN Y. Low temperature synthesis of NbB<sub>2</sub> nanorods by a solid-state reaction route [J]. *Materials Letters*, 2005, 59: 3550–3552.
- [23] MA J, DU J, WU M, LI G, FENG Z, GUO M, SUN Y, SONG W, LIN M, GUO X. A simple inorganic-solvent-thermal route to nanocrystalline niobium diboride [J]. *Journal of Alloys and Compounds*, 2009, 468: 473–476.
- [24] YEH C L, CHEN W H. A comparative study on combustion synthesis of Nb–B compounds [J]. *Journal of Alloys and Compounds*, 2006, 422: 78–85.
- [25] YEH C L, CHEN W H. Preparation of niobium borides NbB and NbB<sub>2</sub> by self-propagating combustion synthesis [J]. *Journal of Alloys and Compounds*, 2006, 420: 111–116.
- [26] YEH C L, WANG H J. Preparation of borides in Nb–B and Cr–B systems by combustion synthesis involving borothermal reduction of Nb<sub>2</sub>O<sub>5</sub> and Cr<sub>2</sub>O<sub>3</sub> [J]. *Journal of Alloys and Compounds*, 2010, 490: 366–371.
- [27] MORRIS M A, MORRIS D G. Ball-milling of elemental powders—Compound formation and/or amorphization [J]. *Journal of Materials Science*, 1991, 26: 4687–4696.
- [28] IIZUMI K, SEKIYA C, OKADA S, KUDOU K, SHISHIDO T. Mechanochemically assisted preparation of NbB<sub>2</sub> powder [J]. *Journal of the European Ceramic Society*, 2006, 26: 635–638.
- [29] JAFARI M, TAJIZADEGAN H, GOLABGIR M H, CHAMI A, TORABI O. Investigation on mechanochemical behavior of Al/Mg–B<sub>2</sub>O<sub>3</sub>–Nb system reactive mixtures to synthesize niobium diboride [J]. *International Journal of Refractory Metals and Hard Materials*, 2015, 50: 86–92.
- [30] TORABI O, NAGHIBI S, GOLABGIR M H, TAJIZADEGAN H, JAMSHIDI A. Mechanochemical synthesis of NbC–NbB<sub>2</sub> nanocomposite from the Mg/B<sub>2</sub>O<sub>3</sub>/Nb/C powder mixtures [J]. *Ceramics International*, 2015, 41: 5362–5369.
- [31] SURYANARAYANA C. Mechanical alloying and milling [J]. *Progress in Materials Science*, 2001, 46: 1–184.
- [32] MURTY B S, RANGANATHAN S. Novel materials synthesis by mechanical alloying-milling [J]. *International Materials Reviews*, 1998, 43: 101–141.
- [33] TAKACS L. Self-sustaining reactions induced by ball milling [J]. *Progress in Materials Science*, 2002, 47: 355–414.
- [34] WIECZOREK-CIUROWA K, OLESZAK D, GAMRAT K. Mechanochemical synthesis and process characterization of some nanostructured intermetallics-ceramics composites [J]. *Journal of Alloys and Compounds*, 2007, 434–435: 501–504.
- [35] CHEN Y, HWANG T, MARSH M, WILLIAMS J S. Study on mechanism of mechanical activation [J]. *Materials Science and Engineering A*, 1997, 226–228: 95–98.

## 采用混合 Nb<sub>2</sub>O<sub>5</sub>, B<sub>2</sub>O<sub>3</sub> 和 Mg 粉末冶金法合成硼化铌

Özge Balcı, Duygu Ağaoğulları, M. Lütfi Öveçoğlu, İsmail Duman

Faculty of Chemical and Metallurgical Engineering, Department of Metallurgical and Materials Engineering, Particulate Materials Laboratories, İstanbul Technical University, Ayazağa Campus, 34469 Maslak, İstanbul, Turkey

**摘要:** 在强还原剂条件下, 以相关的金属氧化物为原材料, 采用粉末冶金法成功合成具有不同含量 NbB、NbB<sub>2</sub> 和 Nb<sub>3</sub>B<sub>4</sub> 相的硼化铌粉末和单相 NbB 粉末。在室温下使用高能球磨机球磨 Nb<sub>2</sub>O<sub>5</sub>、B<sub>2</sub>O<sub>3</sub> 和 Mg 混合粉末。随后, 利用 HCl 浸出除去球磨粉末中无用的 MgO 相, 合成最终产物 NbB–NbB<sub>2</sub>–Nb<sub>3</sub>B<sub>4</sub>, 产物在 1500 °C 下退火 4 h, 以便观察硼化物之间的转换。采用 XRD、DSC、PSA、SEM/EDX、TEM 和 VSM 表征该产物。研究球磨时间(达 9 h)对产物形成、显微组织和热行为的影响。化学计量混合粉末经 2 h 球磨后, 发生了还原反应。在不存在任何二次相和杂质时, 通过机械化学法, 球磨 5 h 并采用 4 mol/L HCl 浸出, 得到高纯纳米尺寸 NbB–NbB<sub>2</sub>–Nb<sub>3</sub>B<sub>4</sub> 粉末。经退火处理后, 纯的纳米尺寸 NbB–NbB<sub>2</sub>–Nb<sub>3</sub>B<sub>4</sub> 粉末转变为单相 NbB, 不存在 NbB<sub>2</sub> 和 Nb<sub>3</sub>B<sub>4</sub> 相。

**关键词:** 硼化铌粉末; 粉末冶金; 机械化学合成; 退火; 组织

(Edited by Xiang-qun LI)